

# Device-independent Quantum Fingerprinting for Large Scale Localization

Ahmed Shokry

Dept. of Computer Science and Engineering  
American University in Cairo  
Cairo, Egypt  
ahmed.shokry@aucegypt.edu

Moustafa Youssef

Dept. of Computer Science and Engineering  
American University in Cairo & Alexandria University  
Cairo, Egypt  
moustafa-youssef@aucegypt.edu

**Abstract**—Although RF fingerprinting is one of the most commonly used techniques for localization, deploying it in a ubiquitous manner requires addressing the challenge of supporting a large number of heterogeneous devices and their variations. We present *QHFP*, a device-independent quantum fingerprint matching algorithm that addresses two of the issues for realizing worldwide ubiquitous large-scale location tracking systems: storage space and running time as well as devices heterogeneity. In particular, we present a quantum algorithm with a complexity that is exponentially better than the classical techniques, both in space and running time. *QHFP* also has provisions for handling the inherent localization error due to building the large-scale fingerprint using heterogeneous devices. We give the details of the entire system starting from extracting device-independent features from the raw RSS, mapping the classical feature vectors to their quantum counterparts, and showing a quantum cosine similarity algorithm for fingerprint matching.

We have implemented our quantum algorithm and deployed it in a real testbed using the IBM Quantum machine simulator. Results confirm the ability of *QHFP* to obtain the correct estimated location with an exponential improvement in space and running time compared to the traditional classical counterparts. In addition, the proposed device-independent features lead to more than 20% better accuracy in median error. This highlights the promise of our algorithm for future ubiquitous large-scale worldwide device-independent fingerprinting localization systems.

**Index Terms**—quantum computing, device-independent location determination systems, practical quantum algorithms, quantum location determination, next generation location tracking systems, quantum pervasive algorithms and systems.

## I. INTRODUCTION

Recent years have witnessed the advent of the field of quantum computing (QC), with a variety of large corporations and startups investing in quantum computing [14], [15], [27]. QC algorithms can solve problems that are infeasible to be solved by classical computers [17], providing exponential gains in some cases [25]. This opens the door for investigating quantum algorithms advantages in new fields such as worldwide location tracking.

Large-scale worldwide fingerprinting localization are commonly used indoor [2], [6], [7], [29] and outdoor [1], [3], [5], [20], [22] due to their accuracy. The fingerprinting techniques work in two phases: the offline RF fingerprint building phase

and the online tracking phase. In the offline phase, the received signal strength (RSS) coming from the different reference points (RPs<sup>1</sup>) in the environment are recorded at the different discrete locations. In the online phase, the RSS coming from RPs at unknown locations are matched against the fingerprint and the closest location in the RSS space becomes the estimated location. However, when the training devices that are used to build the fingerprint and the test devices that are used for localization during the online phase are different, the system accuracy severely degrades. Hence, deploying such systems on different phone types is not a straightforward task as the RSS readings vary for the different kinds of phones, even at the same location and time. This problem, which is known as the device heterogeneity problem [11]–[13], [18], [21], can prevent ubiquitous large-scale fingerprinting-based localization. Moreover, all the traditional fingerprinting techniques need to match the online RSS measurements from the different RPs to the RSS measurements at each fingerprint location, making their time and space complexity  $o(MN)$ , where  $M$  is the number of fingerprint locations and  $N$  is the number of RPs. This can hinder deploying the traditional outdoor/indoor localization in a the large-scale worldwide settings, especially for IoT environments, where the number of RPs in an environment can be significant.

In this paper, we present *QHFP*: a *practical* device-independent quantum fingerprint-based location tracking algorithm that requires space and runs in  $o(M \log(N))$ . We show the details of how to extract device-independent features from the received signal strength measurements, how to construct the quantum fingerprint, how to encode the extracted features in quantum states, and finally; how to calculate the quantum similarity between the online features and the offline ones stored in the fingerprint.

We validate our quantum algorithm in a real testbed. In addition, we quantify its performance using simulations on an IBM quantum computer. The results show the ability of *QHFP* to correctly obtain the estimated location with the same accuracy as its classical counterparts. This comes with an *exponential* enhancement compared to the traditional classical

<sup>1</sup>These reference points can be, e.g., WiFi access points; cellular cell towers; or Bluetooth beacons.

fingerprinting techniques in *both space and time*. In addition, *QHFP* provides 20% enhancement in median localization error in addressing the heterogeneity problem.

The remaining sections are organized as follow: we begin with a brief background on quantum computing in Section II. Section III provides the details of our device-independent quantum fingerprint localization algorithm. Details of the implementation and evaluation results are presented and discussed in Sections IV. Finally, Section V concludes the paper.

## II. BACKGROUND ON QUANTUM COMPUTING

In this section, we give a brief background on the basic concepts of quantum computing that we will build on in the rest of the paper [23], [24].

A quantum bit (qubit) is the basic unit of information and is analogue to the classical bit. Contrary to classical bits, a qubit can exist in a **superposition** of the zero and one states. This superposition is what allows quantum computations to work on both states at the same time. This is often referred to as quantum parallelism. Qubits can have various physical implementations, e.g. the polarization of photons.

Formally, the Dirac notation is commonly used to describe the state of a qubit as  $|\psi\rangle = \alpha|0\rangle + \beta|1\rangle$ , where  $\alpha$  and  $\beta$  are complex numbers called the amplitudes of classical states  $|0\rangle$  and  $|1\rangle$ , respectively. The state of the qubit is normalized, i.e.  $\alpha^2 + \beta^2 = 1$ . When the state  $|\psi\rangle$  is measured, only one of  $|0\rangle$  or  $|1\rangle$  is observed, with probability  $\alpha^2$  and  $\beta^2$ , respectively. The measurement process is destructive, in the sense that the state collapses to the value  $|0\rangle$  or  $|1\rangle$  that has been observed, losing the original amplitudes  $\alpha$  and  $\beta$  [17].

Operations on qubits are usually represented by gates, similar to a classical circuit. An example of a common quantum gate is the NOT gate (also called Pauli-X gate) that is analogous to the not gate in classical circuits. In particular, when we apply the NOT gate to the state  $|\psi_0\rangle = \alpha|0\rangle + \beta|1\rangle$ , we get the state  $|\psi_1\rangle = \beta|0\rangle + \alpha|1\rangle$ . Gates are usually represented by unitary matrices while states are represented by column vectors<sup>2</sup>. The matrix for the NOT gate is  $\begin{bmatrix} 0 & 1 \\ 1 & 0 \end{bmatrix}$  and the above operation can be written as  $|\psi_1\rangle = \text{NOT}(|\psi_0\rangle) = \begin{bmatrix} 0 & 1 \\ 1 & 0 \end{bmatrix} \begin{bmatrix} \alpha \\ \beta \end{bmatrix}$ .

Another important gate is the Walsh–Hadamard gate,  $H$ , that maps  $|0\rangle$  to  $\frac{1}{\sqrt{2}}(|0\rangle + |1\rangle)$ , i.e. a superposition state with equal probability for  $|0\rangle$  and  $|1\rangle$ ; and maps  $|1\rangle$  to  $\frac{1}{\sqrt{2}}(|0\rangle - |1\rangle)$ . Figure 1 shows a simple quantum circuit. Single lines carry quantum information while double lines carry classical information (typically after measurement). The simple circuit applies an  $H$  gate to state  $|0\rangle$ , which produces the state  $\frac{1}{\sqrt{2}}(|0\rangle + |1\rangle)$  at the output of the gate. The measurement step produces either 0 or 1 with equal probability (the squared amplitude of the measured state). The state collapses to the observed classical bit value.

<sup>2</sup>The ket notation  $|\cdot\rangle$  is used for column vectors while the bra notation  $\langle\cdot|$  is used for row vectors.

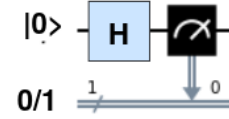
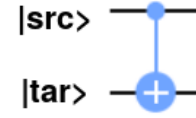
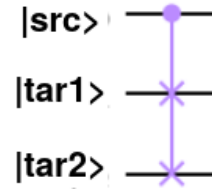


Fig. 1: An example of quantum circuit. Single lines represent quantum information and double lines represent classical information.



(a) The CNOT gate.



(b) The CSWAP gate.

Fig. 2: Simple controlled gates. (a) The NOT gate is applied to the target qubit, if and only if, the source qubit is  $|1\rangle$ . (b) The two target qubits are swapped, if and only if, the source qubit is  $|1\rangle$ .

It is important to note that the concept of quantum **interference** is at the core of quantum computing. Using quantum interference, one uses gates to cleverly and intentionally bias the content of the qubits towards the needed state, hence achieving a specific computation result.

The notion of qubit can be extended to higher dimensions using a quantum register. A quantum register  $|\psi\rangle$ , consisting of  $n$  qubits, lives in a  $2^n$ -dimensional complex Hilbert space  $\mathcal{H}$ . Register  $|\psi\rangle = \sum_0^{2^n-1} \alpha_i |i\rangle$  is specified by complex numbers  $\alpha_0, \dots, \alpha_{2^n-1}$ , where  $\sum |\alpha_i|^2 = 1$ . Basis state  $|i\rangle$  denotes the binary encoding of integer  $i$ . We use the tensor product  $\otimes$  to compose two quantum systems. For example, we can compose the two quantum states  $|\psi\rangle = \alpha|0\rangle + \beta|1\rangle$  and  $|\phi\rangle = \gamma|0\rangle + \delta|1\rangle$  as  $|\omega\rangle = |\psi\rangle \otimes |\phi\rangle = \alpha\gamma|00\rangle + \alpha\delta|01\rangle + \beta\gamma|10\rangle + \beta\delta|11\rangle$ .

Controlled gates act on multiple qubits, where one or more qubits act as a control for some operation on the other qubits (Figure 2). Figure 2a illustrates the controlled NOT gate (CNOT). When the source qubit is  $|1\rangle$ , the NOT operation will be applied to the target qubit. Figure 2b further shows the

controlled SWAP gate (CSWAP) with three qubits as input. In the CSWAP gate, the swap operation is performed on the target wires, if and only if, the source line is  $|1\rangle$ . This can be used to “entangle” qubits together. Entangled qubits are correlated with one another, in the sense that information on one qubit will reveal information about the other unknown qubit, even if they are separated by large distance [17].

A common way to describe a quantum algorithm is to use a quantum circuit, which is a combination of the quantum gates (e.g as in Figure 1). The input to the circuit is a number of qubits (in quantum registers) and the gates act on them to change the combined circuit state using superposition, entanglement, and interference to reach a desired output state that is a function of the algorithm output. The final step is to measure the output state(s), which reveals the required information.

### III. QHFP: A DEVICE-INDEPENDENT QUANTUM FINGERPRINTING LOCALIZATION SYSTEM

In this section, we present the detailed description of our *QHFP* quantum device-independent fingerprinting localization algorithm.

The fingerprinting techniques work in two phases: the offline RF fingerprint building phase and the online tracking phase. In the offline phase, the RSS coming from the different RPs in the environment are recorded at the different discrete locations. In the online phase, the RSS coming from RPs at unknown locations are matched against the fingerprint and the closest location in the RSS space becomes the estimated location. Hence, fingerprint localization can capture the relation between RSS coming from the different RPs in the environment and user location [16], [30], [31].

There are different metrics that can be used to match the online RSS with the fingerprint. In our paper, we proposed a quantum algorithm that uses cosine similarity, which is one of the popular approaches usually used to mitigate device heterogeneity effects [10], [28].

We start the section by explaining how to construct the device-independent fingerprint and how to obtain the quantum fingerprint through encoding the offline RSS vectors from the device-independent fingerprint and the online RSS vector in qubits (i.e. state preparation phase). Then, we present the details of the quantum fingerprinting matching algorithm. Finally, we give an example on how the algorithm can work in detail.

#### A. Device-independent Fingerprint Transformation

In this section, we describe two different techniques to handle the devices heterogeneity problem: the power ratio and the power difference. The basic idea is to transform the traditional RSS fingerprint to a device-independent fingerprint.

1) *Power ratio*: This technique assumes that the ratio between the RSS values coming from different cell towers remains the same on the different phones. Hence, it transforms the RSS values (i.e. power) to a relative power. That is, instead

of using the raw RSS from individual RPs in the fingerprint building phase (offline phase) and the raw RSS in the online matching, it uses the ratio of the RP RSS readings from *each pair* of RPs.

More formally, given a RSS features vector  $X = (f_1, f_2, \dots, f_N)$  from  $N$  RPs in the environment, where  $f_i$  is the RSS coming from RP  $i$ , this technique transforms  $X$  to  $X_r = (r_{1,2}, r_{1,3}, \dots, r_{N-1,N})$ , where  $r_{i,j} = \frac{f_i}{f_j}$  and  $|X_r| = \binom{N}{2}$ .

2) *Power difference*: This approach is similar to the previous approach but takes the power difference instead of the power ratio. It assumes that the difference between the RSS values coming from different RPs remains the same on the different phones.

More formally, given a RSS features vector  $X = (f_1, f_2, \dots, f_N)$  from  $N$  cell-towers in the environment, where  $f_i$  is the RSS coming from cell tower  $i$ , this technique transforms  $X$  to  $X_d = (d_{1,2}, d_{1,3}, \dots, d_{N-1,N})$ , where  $d_{i,j} = f_i - f_j$  and  $|X_d| = \binom{N}{2}$ .

In the next subsection, we show how to map these relative *classical* feature vectors into a *quantum* register.

#### B. State Preparation

The state preparation step aims to encode the relative classical RSS vectors, coming from the power ratio/difference, in quantum registers. Next, the quantum fingerprinting matching algorithm is applied between the online RSS register and the offline ones. Assume there are  $N$  RPs in the environment. Therefore, the  $\binom{N}{2}$ -dimensional normalized RSS vector from the  $N$  RPs  $v = (\beta_0, \beta_1, \dots, \beta_{\binom{N}{2}-1})$ ,  $\sum_{i=0}^{\binom{N}{2}-1} \beta_i^2 = 1$ , can be encoded using a quantum register  $|\delta\rangle$  with  $n = \log(\binom{N}{2})$  qubits. Where  $|\delta\rangle = \sum_{i=0}^{\binom{N}{2}-1} \alpha_i |i\rangle$ , and the basis state  $|i\rangle$  represents the binary encoding of integer  $i$  [9], [26]. Note that the  $\binom{N}{2}$ -dimensional RSS vector can be encoded in  $\log(\binom{N}{2})$  qubits, which is an *exponential saving in the space*.

To perform the state preparation, we used the quantum random access memory (QRAM) which is a popular technique in which the binary code of the RSS measurements vector (i.e.  $\beta_i$ ) is loaded into a qubit register in parallel and conditional rotations are performed to the qubits in the register in order to encode the RSS measurements as amplitudes in the quantum register [9], [19], [26], [32].

We give an example of how to prepare this state from classical vectors later in this section.

#### C. The Quantum Cosine Similarity Algorithm

Figure 3 shows the quantum circuit for calculating the cosine similarity between two normalized RSS vectors coming from applying the RSS power ratio/difference encoded in the quantum registers  $|\delta\rangle$  (e.g. a test RSS vector during the online location tracking phase) and  $|\gamma\rangle$  (e.g. a single fingerprint RSS vector) based on the CSWAP gate [4], [23], [24]. In particular, the circuit calculates:

$$\text{sim}(|\delta\rangle, |\gamma\rangle) = \cos^2(\delta, \gamma) = |\langle \delta | \gamma \rangle|^2 \quad (1)$$

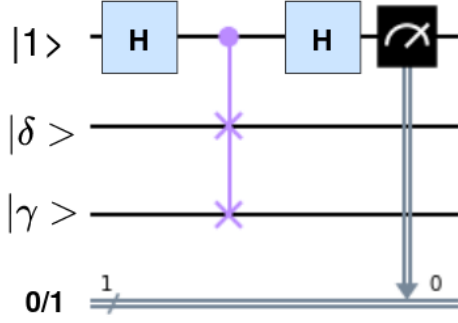


Fig. 3: Quantum fingerprint matching circuit between a single fingerprint RSS vector (encoded in qubit  $\gamma$ ) and the online RSS vector (encoded in qubit  $\delta$ ).

where  $\cos(\delta, \gamma)$  is cosine the angle between the two normalized vectors  $\delta$  and  $\gamma$ . The circuit in Figure 3 takes its input which is the ancilla qubit at state  $|1\rangle$  and the two quantum RSS vectors encoding  $|\delta\rangle$  and  $|\gamma\rangle$ . Then, it applies a series of gates to transform the input to the following joint state,

$$\frac{1}{2} \left( \sqrt{2 - 2|\langle\delta|\gamma\rangle|^2} |0\rangle \frac{|\delta\rangle|\gamma\rangle - |\gamma\rangle|\delta\rangle}{\sqrt{2 - 2|\langle\delta|\gamma\rangle|^2}} + \sqrt{2 + 2|\langle\delta|\gamma\rangle|^2} |1\rangle \frac{|\delta\rangle|\gamma\rangle + |\gamma\rangle|\delta\rangle}{\sqrt{2 + 2|\langle\delta|\gamma\rangle|^2}} \right) \quad (2)$$

Finally, the probability of measuring the top (ancilla) qubit to be 1 is  $\frac{1}{2}(1 + |\langle\delta|\gamma\rangle|^2)$ , which is a function of the required similarity measure between the two vectors. We repeat this circuit  $K$  times to estimate the cosine similarity as  $2 \times \#|1\rangle / K - 1$ . Algorithm 1 explains our device-independent quantum fingerprinting matching algorithm. The  $H$ -gate is applied to the ancilla qubit in order to put it in a superposition state. The CSWAP gate is applied to entangle the ancilla qubit with the training and testing quantum registers. Finally, the  $H$ -gate is applied to generate the desired computation where the probability of receiving  $|1\rangle$  for the ancilla qubit is a function of the required similarity.

#### D. Example

In this section, we illustrate the quantum fingerprint matching algorithm described in the previous section using a simple example with two-values RSS vector. The two normalized RSS vectors to be matched are  $v_1 = (0.43, 0.9)$  and  $v_2 = (0.24, 0.97)$ . Figure 4 shows the complete circuit for calculating the cosine similarity between  $v_1$  and  $v_2$ .

The circuit starts by the state preparation stage, i.e. mapping the RSS vectors  $v_1$  and  $v_2$  to the quantum equivalent  $|\delta\rangle = 0.43|0\rangle + 0.9|1\rangle$  and  $|\gamma\rangle = 0.24|0\rangle + 0.97|1\rangle$ , respectively.

---

#### Algorithm 1 QHFP Fingerprint Matching

---

##### Input:

- 1- Two  $n$ -qubits quantum registers  $|\delta\rangle$  and  $|\gamma\rangle$ , storing RSS vectors of the FP and test locations, coming from the power ratio/difference techniques, to be compared.  $n = \log\binom{N}{2}$ , where  $N$  is the number of RPs.
- 2- An ancilla qubit  $|a\rangle = |1\rangle$
- 3- Number of iterations  $K$ .

##### Output:

Compute an estimate of the similarity between  $|\delta\rangle$  and  $|\gamma\rangle$  as  $|\langle\delta|\gamma\rangle|^2$

- 1: **for**  $k \leftarrow 1$  to  $K$  **do**
  - 2:   Apply  $H(|a\rangle)$
  - 3:   **for**  $i \leftarrow 1$  to  $n$  **do**
  - 4:     Apply CSWAP( $|a\rangle, |\delta_i\rangle, |\gamma_i\rangle$ )
  - 5:   **end for**
  - 6:   Apply  $H(|a\rangle)$
  - 7:    $\eta_k \leftarrow$  measurement of  $|a\rangle$ .
  - 8: **end for**
  - 9: **return**  $\frac{2}{K} \sum_{k=1}^K \eta_k - 1$
- 

This is achieved by using the  $U$  gate, which is represented as,

$$U(\theta) = \begin{bmatrix} \cos(\theta/2) & -\sin(\theta/2) \\ \sin(\theta/2) & \cos(\theta/2) \end{bmatrix} \quad (3)$$

Where  $\theta$  is double the angle between  $|0\rangle$  and the quantum representation of the normalized RSS vector  $|v\rangle$ .

The fingerprint matching part is the same as the one described in Algorithm 1. Since we have only two values in the RSS vectors, the quantum registers contain only one qubit. For the given example, the probability of measuring the first qubit to be in state 1 is 0.9765 and hence the similarity score is 0.9529.

Note that the proposed quantum circuit needs to be repeated for each of the fingerprint locations to determine its similarity score to the test RSS vector. The fingerprint location with the highest score becomes the estimated user location.

## IV. IMPLEMENTATION AND EVALUATION

In this section, we implement the proposed quantum localization algorithm and evaluate its performance in a real testbed.

#### A. Experiment setup

Figure 5 shows our real cellular testbed that spans an  $0.2\text{Km}^2$  outdoor urban area. The area is covered by 8 different cell-towers. Data is collected by war-driving uniformly over the entire area of interest. We also collected an independent test set. Both the fingerprint and test locations are uniformly distributed over the entire area of interest. We use different Android devices for data collection including HTC Nexus One, Prestigio Multipad Wize 3037 3G, HTC One X9 and Motorola Moto G5 plus phones among others. The deployed collector

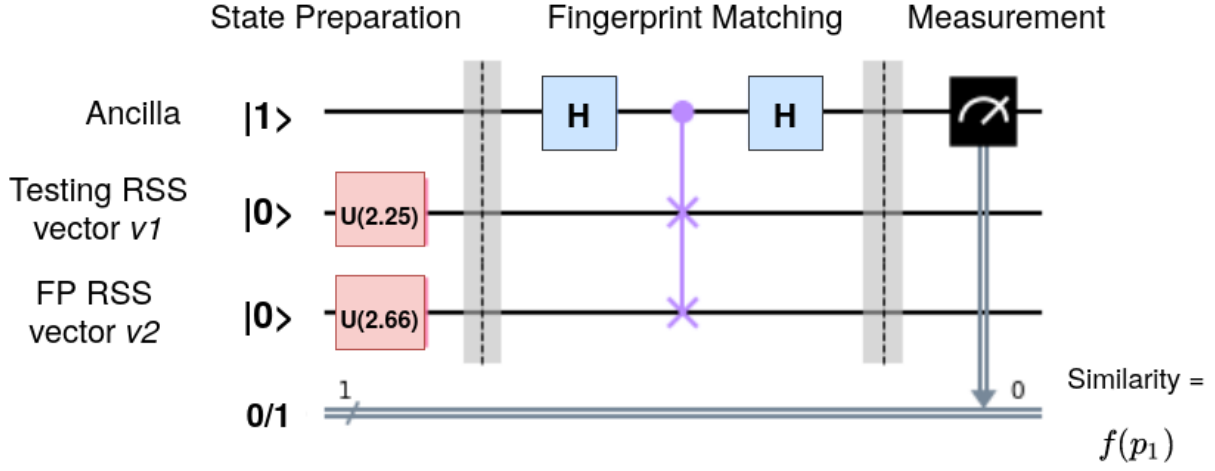


Fig. 4: A detailed example of the quantum fingerprint matching circuit using two-values RSS vectors. The circuit shows the state preparation step, i.e. how to map the testing RSS vector (0.43, 0.9) and training RSS vector (0.24, 0.97) to a quantum state, starting from  $|0\rangle$ .



Fig. 5: The outdoor testbed.

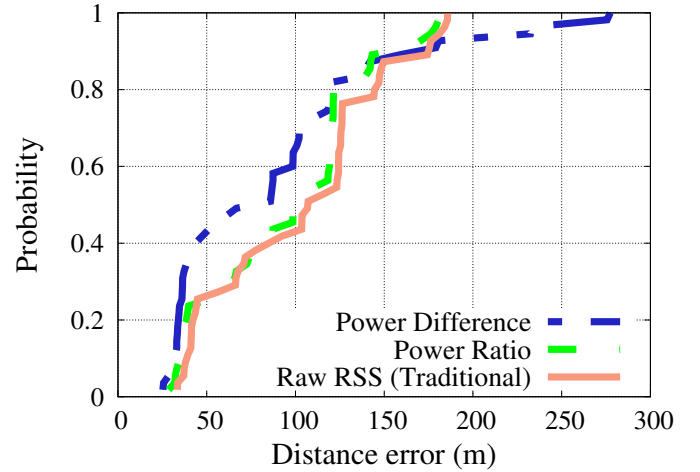


Fig. 6: Effect of device heterogeneity techniques.

software collects GPS ground-truth locations, received signal strengths, and timestamps.

The 8 cell-towers RSS can be encoded in 5 qubits after applying RSS power ratio or difference techniques. Therefore, we require a total of 11 qubits for running the circuit in Figure 3, 10 qubits for encoding the training and testing RSS vectors and one for the Ancilla qubit. We use the IBM quantum machine simulator, which supports up to 28 qubits.

### B. Comparison Between the Different Heterogeneity Handling Techniques

Figure 6 and Table I show a comparison between the traditional raw RSS, the quantum power ratio, and the quantum power difference fingerprinting techniques. Specifically, the results show that *QHFP*, through its heterogeneity handling

techniques, can achieve a better localization accuracy than traditional raw RSS localization by more than 20% in the median error. The results also show that the power difference technique is superior to the power ratio technique. This can be explained by noting that the RSS reported by the phone API is in log-scale.

### C. Comparison with Classical Localization

Figure 7 shows the CDF of distance error for the quantum and classical localization system using the same device-independent features (i.e. after applying the power difference heterogeneity technique). The figure shows that *QHFP* has the same accuracy as the classical one, but with the potential exponential saving in time and space.

TABLE I: Comparison between quantum and classical localization systems error quantiles. Numbers between parenthesis indicate percentage of enhancement over raw RSS.

System	Q1	Median	Q3
Raw RSS - Traditional	40	103	121
<i>QHFP</i> - Power Ratio	39 (2.6%)	98 (5.1%)	121 (0%)
<i>QHFP</i> - Power Difference	36 (11.1%)	85.5 (20.5%)	119 (1.7%)

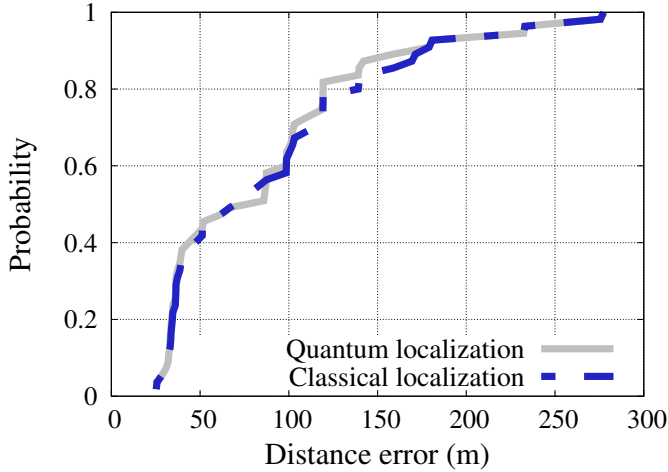


Fig. 7: CDF of localization error for quantum and classical localization using the power difference technique.

#### D. Effect of Number of Shots

Figure 8 shows the impact of increasing the number of algorithm iterations, i.e. re-running the system (parameter  $K$  in Algorithm 1), on the power difference quantum localization accuracy. It is evident from the figure that increasing the number of iterations leads to a better localization accuracy for both techniques till it starts saturating around 4096 shots.

#### E. Discussion

Last section shows that the device-independent fingerprinting localization techniques have accuracy that is better than the traditional raw RSS one in the real testbed used in our experiments.

The device-independent classical version of the localization system requires  $o(N^2M)$  space and matching runs in  $o(N^2M)$ , for  $N$  RPs and  $M$  fingerprint locations. On the other hand, *QHFP* requires  $o(M \log N)$  for both space and time. This is an exponential enhancement in both space and running time. Figure 9 explains how the running time complexity for the quantum and the classical localization systems scale with the increase of the number of RPs for a fixed number of locations in the fingerprint. The figure confirms the **exponential saving in running time** of the proposed quantum algorithm. This is important in many scenarios such as worldwide localization and IoT applications, where there

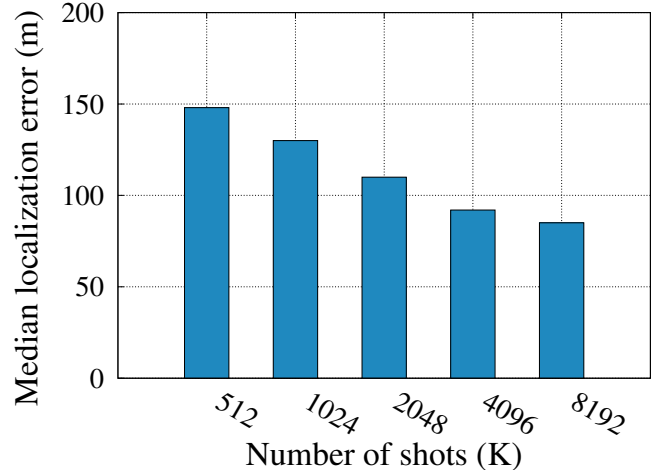


Fig. 8: Effect of number of shots on the quantum power difference localization error.

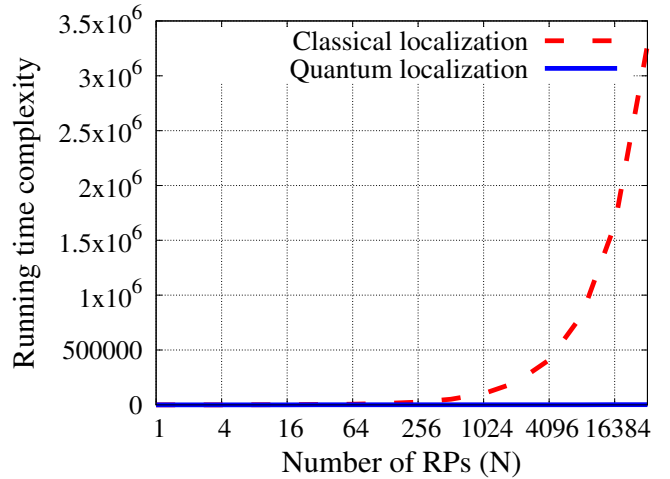


Fig. 9: Running time complexity for the quantum and the classical algorithms.

are a lot of RPs with different technologies (cellular, WiFi, BT, etc). Moreover, in order to get a better accuracy, one needs to fuse the signal coming from the significant number of RPs in the environment. Hence, the exponential saving in time and space becomes a must.

*QHFP* is not only useful for the online fingerprint matching process but also for offline state preparation (quantum fingerprint construction) as it can reduce the size of the fingerprint RSS vectors from  $o(N^2)$  to  $o(\log(N))$ . This is important not only to speed up the matching process but also to save the space required for downloading and storing the large-scale worldwide fingerprint from the server to mobile phones if the fingerprint matching is performed on the mobile phones. In addition, quantum co-processors (similar to GPUs) have started to appear [8] which can enable quantum localization on mobile devices.

Finally, the space and time complexity of *QHFP* can be re-



duced to  $o(\log(NM))$  by encoding all the fingerprint locations data in one circuit. This might have a significant implications to several localization and spatial algorithms.

## V. CONCLUSION

In this paper, we have presented, *QHFP*, a practical device-independent quantum fingerprinting algorithm. *QHFP* can provide high accuracy localization with different phone types while leading to an exponential saving in the space and the running time of the current fingerprinting localization systems. Results from deploying *QHFP* in a real testbed confirm its advantages compared to the traditional classical techniques. Moreover, the proposed device-independent features achieves a median distance error of 85.5m, which is 20% better than the traditional fingerprinting methods.

Currently, we are exploring different quantum similarity metrics, obtaining theoretical quantum bounds on performance, and optimizing other spatial algorithms using quantum computing.

## REFERENCES

- [1] Heba Aly, Anas Basalamah, and Moustafa Youssef. Lanequest: An accurate and energy-efficient lane detection system. In *2015 IEEE International Conference on Pervasive Computing and Communications (PerCom)*, pages 163–171. IEEE, 2015.
- [2] Heba Aly and Moustafa Youssef. New insights into wifi-based device-free localization. In *Proceedings of the 2013 ACM conference on Pervasive and ubiquitous computing adjunct publication*, pages 541–548, 2013.
- [3] Heba Aly and Moustafa Youssef. semMatch: Road semantics-based accurate map matching for challenging positioning data. In *Proceedings of the 23rd SIGSPATIAL International Conference on Advances in Geographic Information Systems*, pages 1–10, 2015.
- [4] Harry Buhrman, Richard Cleve, John Watrous, and Ronald De Wolf. Quantum Fingerprinting. *Physical Review Letters*, 87(16):167902, 2001.
- [5] Gu Chen, Ahmed Shokry, and Moustafa Youssef. The Effect of Ground Truth Accuracy on the Evaluation of Localization Systems. *IEEE INFOCOM*, 2021.
- [6] Rizanne Elbakly and Moustafa Youssef. A robust zero-calibration RF-based localization system for realistic environments. In *2016 13th Annual IEEE International Conference on Sensing, Communication, and Networking (SECON)*, pages 1–9. IEEE, 2016.
- [7] Moustafa Elhamshary and Moustafa Youssef. Towards Ubiquitous Indoor Spatial Awareness on a Worldwide Scale. *SIGSPATIAL Special*, 9(2):36–43, 2017.
- [8] George J Frangou, Stephane Chretien, and Ivan Rungger. The first quantum co-processor hybrid for processing quantum point cloud multimodal sensor data. *Proceedings of the Future Technologies Conference*, pages 411–426, 2019.
- [9] Vittorio Giovannetti, Seth Lloyd, and Lorenzo Maccone. Quantum Random Access Memory. *Phys. Rev. Lett.*, 100:160501, Apr 2008.
- [10] S. Han, C. Zhao, W. Meng, and C. Li. Cosine Similarity based Fingerprinting Algorithm in WLAN Indoor Positioning against Device Diversity. *2015 IEEE International Conference on Communications (ICC)*, pages 2710–2714, 2015.
- [11] Mohamed Ibrahim and Moustafa Youssef. CellSense: A probabilistic RSSI-based GSM positioning system. In *2010 IEEE Global Telecommunications Conference GLOBECOM 2010*, pages 1–5. IEEE, 2010.
- [12] Mohamed Ibrahim and Moustafa Youssef. CellSense: An accurate energy-efficient GSM positioning system. *IEEE Transactions on Vehicular Technology*, 61(1):286–296, 2011.
- [13] Mohamed Ibrahim and Moustafa Youssef. Enabling wide deployment of GSM localization over heterogeneous phones. In *2013 IEEE International Conference on Communications (ICC)*, pages 6396–6400. IEEE, 2013.
- [14] Julian Kelly. A preview of Bristlecone, Google’s New Quantum Processor. *Google Research Blog*, 5, 2018.
- [15] Will Knight. IBM raises the Bar with a 50-qubit Quantum Computer. *Sighted at MIT Review Technology*, 2017.
- [16] Nesma Mohssen, Rana Momtaz, Heba Aly, and Moustafa Youssef. It’s the human that matters: Accurate user orientation estimation for mobile computing applications. *Mobiquitous*, 2014.
- [17] Michael A. Nielsen and Isaac L. Chuang. *Quantum Computation and Quantum Information*. Cambridge University Press, USA, 10th edition, 2011.
- [18] Jun-geun Park, Dorothy Curtis, Seth Teller, and Jonathan Ledlie. Implications of Device Diversity for Organic Localization. pages 3182–3190. IEEE, 2011.
- [19] Patrick Rebentrost, Masoud Mohseni, and Seth Lloyd. Quantum Support Vector Machine for Big Data Classification. *Physical review letters*, 113(13):130503, 2014.
- [20] Ahmed Shokry, Mostafa Mahmoud Elhamshary, and Moustafa Youssef. DynamicSLAM: Leveraging Human Anchors for Ubiquitous Low-overhead Indoor Localization. *IEEE Transactions on Mobile Computing*, 2020.
- [21] Ahmed Shokry, Moustafa Elhamshary, and Moustafa Youssef. The Tale of Two Localization Technologies: Enabling Accurate Low-overhead WiFi-based Localization for Low-end Phones. *ACM SIGSPATIAL*, pages 1–10, 2017.
- [22] Ahmed Shokry, Marwan Torki, and Moustafa Youssef. DeepLoc: a Ubiquitous Accurate and Low-overhead Outdoor Cellular Localization System. *Proceedings of the 26th ACM SIGSPATIAL International Conference on Advances in Geographic Information Systems*, pages 339–348, 2018.
- [23] Ahmed Shokry and Moustafa Youssef. Quantum Computing for Location Determination. *arXiv preprint arXiv:2106.11751*, 2021.
- [24] Ahmed Shokry and Moustafa Youssef. Towards Quantum Computing for Location Tracking and Spatial Systems. pages 278–281, 2021.
- [25] Peter W Shor. Polynomial-time Algorithms for Prime Factorization and Discrete Logarithms on a Quantum Computer. *SIAM review*, 41(2):303–332, 1999.
- [26] Andrei N. Soklakov and Rüdiger Schack. Efficient State Preparation for a Register of Quantum Bits. *Phys. Rev. A*, 73:012307, Jan 2006.
- [27] Swamit S Tannu and Moinuddin K Qureshi. A Case for Variability-aware Policies for Nisq-era Quantum Computers. *arXiv preprint arXiv:1805.10224*, 2018.
- [28] Qing Yang, Shijue Zheng, Ming Liu, and Yawen Zhang. Research on Wi-Fi Indoor Positioning in a Smart Exhibition Hall based on Received Signal Strength Indication. *EURASIP Journal on Wireless Communications and Networking*, 2019(1):275, Dec 2019.
- [29] Moustafa Youssef. Towards Truly Ubiquitous Indoor Localization on a Worldwide Scale. *Proceedings of the 23rd SIGSPATIAL International Conference on Advances in Geographic Information Systems*, pages 1–4, 2015.
- [30] Moustafa Youssef and Ashok Agrawala. The Horus WLAN Location Determination System. pages 205–218, 2005.
- [31] Moustafa Youssef and Ashok Agrawala. Location-clustering techniques for WLAN location determination systems. *International Journal of Computers and Applications*, 28(3):278–284, 2006.
- [32] Zhikuan Zhao, Jack K Fitzsimons, and Joseph F Fitzsimons. Quantum-assisted Gaussian Process Regression. *Physical Review A*, 99(5):052331, 2019.